
000 001 002 003 004 005 006 007 008 009 010 011 012 013 014 015 016 017 018 019 020 021 022 023 024 025 026 027 028 029 030 031 032 033 034 035 036 037 038 039 040 041 042 043 044 045 046 047 048 049 050 051 052 053 SAFEDEC: CONSTRAINED DECODING FOR SAFE AU- TOREGRESSIVE GENERALIST ROBOT POLICIES

Anonymous authors

Paper under double-blind review

ABSTRACT

Recent advances in end-to-end, multi-task robot policies based on transformer models have demonstrated impressive generalization to real-world embodied AI tasks. Trained on vast datasets of simulated and real-world trajectories, these models map multimodal observations directly to action sequences for physical execution. Despite promising real-world capabilities, these models are still data-driven and, therefore, lack explicit notions of behavioral correctness. We address this gap by introducing **SafeDec**, a constrained decoding framework for autoregressive, transformer-based robot policies that enforces invariant safety specifications on candidate action trajectories. Task-specific safety rules are expressed as Signal Temporal Logic (STL) formulas and are enforced at inference time with minimal overhead. Our method ensures that generated actions provably satisfy STL specifications under assumed dynamics at runtime without retraining, while remaining agnostic of the underlying policy. We evaluate **SafeDec** on tasks from the CHORES benchmark for state-of-the-art generalist policies (e.g., SPOC, Flare, PoliFormer) across hundreds of procedurally generated environments and show that our decoding-time interventions are useful not only for filtering unsafe actions but also for conditional action generation. Videos are available at **constrained-robot-fms.github.io**.

1 INTRODUCTION

Recent advances in developing large transformer-based models for robotics have enabled general-purpose policies that map multi-modal inputs such as RGB images, natural language instructions, and proprioceptive inputs to action sequences (Hu et al., 2023). Shortest Path Oracle Clone (SPOC) (Ehsani et al., 2024), PoliFormer (Zeng et al., 2025), Flare (Hu et al., 2025) and OpenVLA (Kim et al., 2024) exhibit impressive generalization in navigation and manipulation tasks and serve as versatile robot controllers for real-world deployment contexts. However, these models are primarily data-driven and lack any explicit notion of safety. Although these models may implicitly exhibit safety-related behaviors depending on the patterns in their training data, there is no formal guarantee that models will consistently behave safely in all situations. This serves as a limiting factor for deploying these foundation models in the physical world where rule compliance and regulatory safety rule adherence are crucial.

Formal specifications have long been used to specify safety requirements for robotic deployments (Menghi et al., 2019; Farrell et al., 2018). Temporal logics (TL) (Pnueli, 1977) can capture safety constraints on robot behavior, such as “remain within the permitted region zones and avoid dangerous obstacles”. Although TL has seen success in classical robotic planning for safety constraint satisfaction, its use for enforcing safety for large transformer-based robot policies remains limited. Additionally, retraining or fine-tuning these large pre-trained models to directly embed temporal logic specification is challenging (Kapoor et al., 2024). First, retraining models is a costly endeavor in terms of computational resources and data requirements. Moreover, due to the stochastic nature of these models, it is difficult to guarantee strict satisfaction of safety constraints through training alone. Hence, there is a pressing need for methods that can enforce safety specifications efficiently at inference time without disrupting the model’s pre-trained behavior.

In the field of natural language processing, syntactic constraints have been successfully enforced by applying constrained decoding at inference time (Willard & Louf, 2023; Beurer-Kellner et al.,

054 2023; AI, 2023). These approaches typically mask out tokens that violate a syntactic constraint
 055 defined over token sequences. For example, regular expressions (regex) represent a widely used
 056 form of syntactic constraint, requiring that generated token sequences conform to predefined struc-
 057 tural patterns (Willard & Louf, 2023; Beurer-Kellner et al., 2023). Inspired by this line of work,
 058 we extend the paradigm of constrained decoding to enforce safety constraints over action trajec-
 059 tories in dynamical systems and propose *safety specification aligned decoding* (*SafeDec*) for trans-
 060 former based policies that ensures generated action sequences provably satisfy Signal Temporal
 061 Logic (STL) (Maler & Nickovic, 2004a) specifications under assumed dynamics. Our key insight is
 062 that decoding-time interventions can be used not just to filter unsafe actions, but to *condition the gen-*
 063 *eration process itself* on specification satisfaction. This conditioning is critical because it steers the
 064 model toward generating safety specification satisfying actions rather than relying on post hoc rejec-
 065 tion. *SafeDec* reduces risk of infeasible outputs while preserving the original action distribution
 066 of the model. To enforce such specifications, we leverage the formal semantics of STL to evaluate
 067 candidate actions at runtime and mask those that lead to future violations. Our method is agnostic
 068 to the underlying foundation model, requiring only two properties: (1) access to the decoding-layer
 069 logits during inference, and (2) access to an approximate dynamics model to predict future states. To
 070 efficiently evaluate STL specifications at inference time, we use a high-performance computational
 071 graph based library *STLCG++* (Kapoor et al., 2025c). In this work, we focus on safety enforcement
 072 for navigation policies in indoor environments, and leave extension to manipulation settings for fu-
 073 ture work. We also focus on STL specifications without liveness operators as they capture a large
 074 class of safety constraints in robot learning (He et al., 2024; Yun et al., 2025; Kapoor et al., 2025b;
 075 Zhao et al., 2024). To the best of our knowledge, this is the first work to enforce formal safety on
 076 transformer-based robotic policies at inference time using constrained decoding.

077 Our main contributions are as follows: First, we formalize the general problem of enforcing safety
 078 constraints during inference for autoregressive robot policies. In this work, we use STL to represent
 079 safety requirements because it is expressive over continuous states and provides quantitative robust-
 080 ness. Additionally, we focus on transformer-based autoregressive policies given their widespread
 081 adoption. Second, we propose an inference-time technique that reweights or masks candidate actions
 082 using STL satisfaction scores in (Section 3.2 and 3.3). Finally, we demonstrate the effectiveness of
 083 our method on state-of-the-art object navigation models without modifying model parameters (Sec-
 084 tion 4).

085
 086 **2 PRELIMINARIES**

087
 088 **2.1 SIGNAL TEMPORAL LOGIC**

089
 090 Signal Temporal Logic (STL) is an expressive framework for defining properties and reasoning over
 091 continuous time real-valued (Maler & Nickovic, 2004b). Formally, $(s, t) \models \phi$ denotes that a signal
 092 s satisfies the STL formula ϕ at time t . An atomic predicate of an STL formula is represented by
 093 inequalities of the form $\mu(s(t)) > 0$. The truth value of the predicate μ is equivalent to $\mu(s(t)) > 0$.
 094 Note that with slight abuse of notation, μ represents both the predicate and a function of the trajectory
 095 $s(t)$. Any STL formula consists of Boolean and temporal operations on these predicates, and the
 096 syntax of STL formulas is defined recursively as follows:

097
 098
$$\phi := \mu \mid \neg\mu \mid \phi \wedge \psi \mid \phi \vee \psi \mid \mathbf{G}_{[a,b]} \psi \mid \mathbf{F}_{[a,b]} \psi \mid \phi \mathbf{U}_{[a,b]} \psi$$

099
 100
 101 where ψ and ϕ are STL formulae, \mathbf{G} denotes the globally operator, \mathbf{F} the eventually operator, and
 102 \mathbf{U} is the until operator. For example, $s \models \mathbf{G}_{[a,b]} \psi$ specifies that ψ must be in all times in the given
 103 interval, $t \in [a, b]$ of the signal s . Similarly, the operator *until* in $s \models \phi \mathbf{U}_{[a,b]} \psi$ defines that ϕ must
 104 be true until ψ becomes true within a time interval $[a, b]$.

108 Given a signal s_t representing a signal starting at time t , the Boolean semantics of satisfaction of
109 $s_t \models \phi$ are defined inductively as follows:
110

$$\begin{aligned} s_t \models \mu &\iff \mu(s(t)) > 0 \\ s_t \models \neg\varphi &\iff \neg(s_t \models \varphi) \\ s_t \models \varphi_1 \wedge \varphi_2 &\iff (s_t \models \varphi_1) \wedge (s_t \models \varphi_2) \\ s_t \models F_{[a,b]}(\varphi) &\iff \exists t' \in [t+a, t+b] \text{ s.t. } s_{t'} \models \varphi \\ s_t \models G_{[a,b]}(\varphi) &\iff \forall t' \in [t+a, t+b] \text{ s.t. } s_{t'} \models \varphi \end{aligned}$$

117 Apart from the Boolean semantics, quantitative semantics are defined for a signal to compute a real-
118 valued metric indicating *robustness*, i.e., the strength of satisfaction or violation. For the sake of
119 brevity, the definition of robustness is provided in Appendix A.1.
120

121 2.2 CONSTRAINED DECODING IN TRANSFORMERS

122

123 A large variety of autoregressive transformer-based models generate final outputs by producing a
124 probability distribution over the model vocabulary at each timestep. This distribution is generated
125 by performing a softmax operation over the model’s last hidden layer. Then, through the process of
126 *decoding*, tokens are selected to maximize the overall likelihood of an output sequence. In standard
127 decoding, this maximization can be performed by either greedily selecting the most probable token
128 at each step or by using a beam search to maintain multiple high-likelihood candidates. However,
129 this often leads to degenerate output sequences that are repetitive (Holtzman et al., 2019). A common
130 approach is to use sampling strategies like top k (Fan et al., 2018), and nucleus sampling (Holtzman
131 et al., 2019) that introduce stochasticity to encourage more diverse outputs. Constrained decoding
132 (Hokamp & Liu, 2017) modifies this probabilistic selection by pruning invalid tokens to ensure
133 that the generated sequences satisfy predefined constraints. These constraints are often syntactic,
134 such as regular expressions, JSON formatting, or programming language grammars (Welleck et al.,
135 2024). There is also recent work on enforcing *semantic* constraints that ensure coherence of the
136 output or alignment with specific knowledge bases (Peyrard et al., 2024). Formally, constrained
137 decoding can be seen as maximizing the probability of the output sequence subject to a constraint
 \mathcal{C} : $\arg \max_{y \in \mathcal{Y}_C} P(y | x)$ where \mathcal{Y}_C is the set of sequences satisfying \mathcal{C} .
138

139 3 SPECIFICATION-GUIDED CONSTRAINED DECODING

140

141 In this section, we introduce a novel problem formulation for `SafeDec` in autoregressive
142 transformer-based robot policies. First, we highlight the challenge in specification checking for
143 these policies in contrast to traditional syntactical constraint checking adopted by LLMs, and our so-
144 lution to remedy it. Then, we propose two novel inference-time techniques for specification aligned
145 decoding: *Hard Constrained Decoding (HCD)* and *Robustness Constrained Decoding (RCD)*.
146

147 3.1 PROBLEM STATEMENT

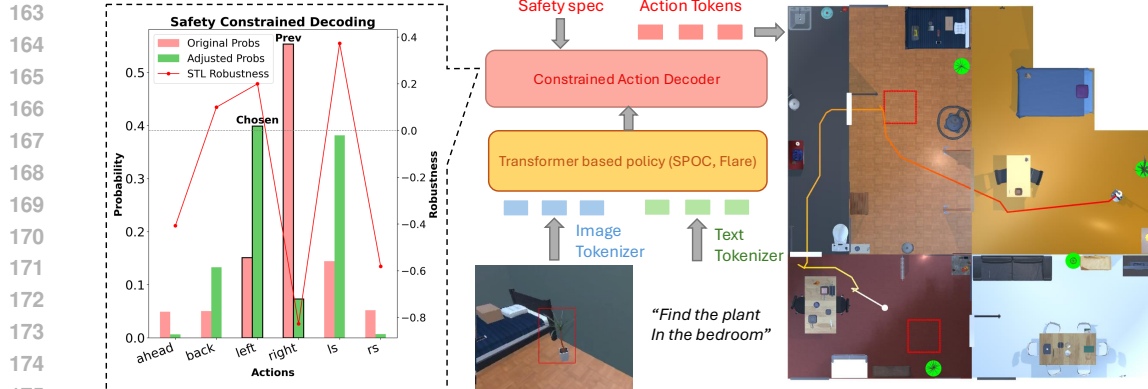
148

149 As highlighted in the background section, existing techniques in constrained decoding for language
150 models enforce *syntactic constraints* defined over tokens, such as conforming to a context-free gram-
151 mar or matching a regular expression. In these setups, constraint checking can be performed in the
152 model’s token space.

153 In contrast, transformer-based policies operate in a physical environment and constraints (captured
154 via temporal logic) are defined over state variables. Since a large class of end-to-end policies solely
155 propose action sequences, specification checking can only be performed as actions are executed
156 and the environment is simulated forward. In this case, constraint checking cannot be done solely
157 in the token space and requires environmental feedback or a dynamics stepping function. Hence,
158 we leverage an approximate first order dynamics function to compute specification satisfaction of
159 different action sequences proposed by these policies.

160 Consider a discrete dynamical system with states $x_t \in \mathbb{R}^n$ and actions $a_t \in \mathbb{A}$ at time step t . The
161 system’s dynamics are defined by $x_{t+1} = f(x_t, a_t)$ where $f : \mathbb{R}^n \times \mathbb{A} \rightarrow \mathbb{R}^n$ maps the current state
($x_t \in \mathbb{R}^n$) and a discrete action ($a_t \in A$) to the next state $x_{t+1} \in \mathbb{R}^n$. This system is controlled by

162



163
164
165
166
167
168
169
170
171
172
173
174
175
176
177
178
179
180
181
182
183
184
185
186
187
188
189
190
191
192
193
194
195
196
197
198
199
200
201
202
203
204
205
206
207
208
209
210
211
212
213
214
215
Figure 1: Overview of our specification aligned decoding framework. Given multimodal observations (RGB images and language goals), a pretrained transformer-based navigation policy (e.g., SPOC, Flare, PoliFormer) generates candidate actions. Our constrained decoder then filters or reweights these actions using robustness scores from a user-defined STL safety specification. **Left:** Original action probabilities (red) from the pretrained policy are modified by SafeDec using STL robustness: actions predicted to violate the safety specification receive reduced weights, while safer actions are boosted. The chosen safe action and adjusted probabilities (green) are highlighted. **Right:** An example navigation episode where the robot starts in the kitchen (white dot) and moves toward the bedroom to locate the target object (green marker middle-right), while avoiding user-defined hazardous regions (red zones) throughout the trajectory.

a policy that selects an action a_t at each time step based on observations and task context such as user-provided natural-language instructions or goal waypoints.

In this work, we focus on robot policies that generate actions based on multi-modal inputs, including sensor observations (e.g., RGB, depth, LiDAR) and natural language instructions. Let \mathcal{I}_t represent the aggregated input at timestep t . Given the history of encoded inputs up to time t , a transformer-based policy parameterized by θ predicts embeddings for the next $T-t$ actions:

$$\{e_{a_{t+k}}\}_{k=1}^{T-t} = \text{Transformer}_\theta(\{e_{\mathcal{I}_\tau}\}_{\tau=0}^t).$$

Each predicted action embedding is decoded into an action $\hat{a}_{t+k} \in \mathbb{A}$, resulting in a predicted action sequence $\{\hat{a}_{t+1}, \dots, \hat{a}_T\}$, where T denotes the planning horizon.

Now, consider that the system is required to satisfy requirements encoded using an STL formula φ defined over the state variables of the system. Formally, the goal is to ensure that the resulting trajectory satisfies the specification φ :

$$\{(x_0, \hat{a}_0), \dots, (x_T, \hat{a}_T)\} \models \varphi$$

Most of the existing techniques for specification enforcement perform posthoc manipulation of proposed actions through filtering or rejecting action sequences that violate the specification φ . Although manipulation after sampling can ensure specification satisfaction, it can lead to distorting the model's learned distribution, producing low-likelihood output. This undermines the inductive biases learned during pretraining and leads to degenerate, brittle behaviors. A similar problem was highlighted when ensuring compliance with logical constraints for large language models (LLM) in Park et al. (2024). Additionally, these models decode actions sequentially, where each action a_t is conditioned on previously generated tokens $a_{<t}$. Posthoc manipulation can disrupt this causal chain and lead to a mismatch between the model's internal hidden state and the executed sequence. Hence, we propose the following problem statement:

How can we enforce temporal logic constraints during action generation in robot foundation models such that the output sequence (1) satisfies an STL specification φ , and (2) remains faithful to the model's autoregressive distribution $\pi(a_{1:T} | \mathcal{I}_{1:T})$?

216 Let $\pi(a_{0:T})$ be the *unconstrained* action-sequence distribution produced by the transformer-based
 217 policy’s decoder (e.g. the softmax over logits generated by the Transformer). We define the ideal
 218 constrained distribution over action sequences as:

$$220 \quad Q_{\pi, \varphi}(a_{0:T}) = \frac{\pi(a_{0:T}) \cdot \mathbf{1}[(x_{1:T}, a_{0:T}) \models \varphi]}{\sum_{a'_{0:T}} \pi(a'_{0:T}) \cdot \mathbf{1}[(x'_{1:T}, a'_{0:T}) \models \varphi]} \quad (1)$$

223 where $x_{1:T}$ denotes the state trajectory induced by the system dynamics under actions $a_{0:T}$ and
 224 $\mathbf{1}[\cdot]$ is the indicator function that returns 1 iff the trajectory-action pair satisfies the specification.
 225 Equation 1 is the exact Bayesian conditioning of π on the event that the generated rollout satisfies φ .
 226 Hence, sampling from $Q_{\pi, \varphi}$ would give sequences that (i) inherit the original model’s preferences
 227 encoded in π and (ii) *guarantee* specification satisfaction.

228 In this work, we propose a technique to overcome the drawbacks of post-hoc safety enforcement
 229 methods (such as filtering) by leveraging constrained decoding techniques. Specifically, we propose
 230 **SafeDec** : A constrained decoding strategy that integrates STL specifications into the foundation
 231 model action selection process itself, ensuring satisfaction while *remaining as close as possible to*
 232 *the base model distribution*.

234 3.2 HARD CONSTRAINED DECODING

236 As highlighted in the background section, in the final layer, predictions are detokenized and a pro-
 237 jection layer converts the embeddings into logits over the vocabulary space. These logits are further
 238 converted into a probability distribution using a softmax operation. In prior work, for structured out-
 239 put generation in LLMs, some invalid tokens are masked based on syntactical constraints or other
 240 criteria (Welleck et al., 2024; Park et al., 2024). This is done by setting their logit value as $-\infty$
 241 before the softmax operation is applied. For HCD, we use a similar approach as constrained decod-
 242 ing literature (Welleck et al., 2024) and mask out predicted action tokens that violate our given STL
 243 specification φ during sequential generation. Formally, to enforce the STL specification φ during
 244 sequential generation, we adjust the logits at each timestep $t + k$ as follows:

245 Let \mathbf{z}_{t+k} denote the logits at timestep $t + k$. For each action choice i at timestep $t + k$, we define:

$$247 \quad z_{t+k}^{(i)} = \begin{cases} -\infty, & \text{if } \hat{x}_{t+k}^{(i)} = f(x_{t+k-1}, \hat{a}_{t+k-1}^{(i)}) \text{ violates } \varphi \\ 248 \quad z_{t+k}^{(i)}, & \text{otherwise} \end{cases}$$

250 Here t is the current decision step, k is an index for the look-ahead step $t + k$ within a planning
 251 horizon of length T ($k \in [1..T]$), $\hat{a}_{t+k}^{(i)}$ is the action mapping to the token i and $\hat{x}_{t+k}^{(i)}$ is the next
 252 state value upon taking this action. This next state is elicited using a simple dynamics model (f) as
 253 highlighted in the previous section. Adjusting logits in this fashion ensures that any invalid token
 254 with respect to the safety specification will have zero probability of being selected after applying the
 255 softmax function.

256 3.3 ROBUSTNESS CONSTRAINED DECODING

259 HCD ensures compliance but can lead to compromising task success, which can be undesirable. A
 260 similar tradeoff was observed by Liu et al. (2021) when probability space-steering preserved model
 261 fluency while reducing toxic continuations compared with hard-filtering strategies that inflated per-
 262 plexity and eroded diversity. Hence, we propose an alternative approach, called RCD, where we
 263 leverage the quantitative semantics of STL specifications (robustness). Unlike HCD, which applies
 264 hard masking to completely remove unsafe actions, RCD softly guides the model toward safer ac-
 265 tions by incorporating robustness scores that reflect the degree of satisfaction of φ . This is similar
 266 to the approach proposed in Liu et al. (2021) where the next-token distributions were re-weighted
 267 based on the utility scores provided by another language model. Our utility scores are quantified by
 268 the robustness function ($\rho(\langle x_0, x_1, \dots, x_t \rangle, \varphi)$) that returns a real-valued score indicating how well
 269 a predicted state satisfies the specification. Positive robustness values denote specification satis-
 270 faction, while negative values capture the degree of violation. A formal definition of robustness in line
 271 with the STL quantitative semantics is provided in Appendix A.1.

270 First, we compute a robustness score for each candidate action: $r_{t+k}^{(i)} =$
 271 $\rho(\langle x_0, x_1, \dots, x_{t+k-1}, \hat{x}_{t+k}^{(i)} \rangle, \varphi)$ where $\rho(\cdot, \varphi)$ is the STL robustness metric, and $\hat{x}_{t+k}^{(i)}$ is the
 272 predicted next state under action $\hat{a}_{t+k}^{(i)}$. This robustness score $r_{t+k}^{(i)}$ quantifies how well each
 273 candidate action satisfies the specification φ . These scores are then converted into weights using
 274 exponential scaling: $w_{t+k,i} = \exp(\alpha \cdot r_{t+k,i})$ where α is a temperature parameter that adjusts the
 275 sharpness of the bias. We use these weights to shift the original logits: $\tilde{z}_{t+k,i} = z_{t+k,i} + \beta \cdot w_{t+k,i}$
 276 where β is a hyperparameter that modulates the trade-off between specification adherence and the
 277 original task objective. Finally, we obtain the action distribution by applying softmax over the
 278 adjusted logits: $p_{t+k} = \text{softmax}(\tilde{\mathbf{z}}_{t+k})$
 279

280 This approach allows for graded preferences that improve flexibility and robustness to dynamics ap-
 281 proximation errors. By ensuring that all actions preserve a non-zero probability, the policy remains
 282 capable of recovering from errors arising from an imperfect dynamics model. Concretely, if the
 283 predicted successor \hat{x}_{t+1} is off by ϵ , an action that appeared marginally unsafe can be safe in the
 284 true system, and vice versa. Retaining a weighted down probability for this action gives the sampler
 285 a fall-back option whereas HCD would completely rule this action out due to 0 probability. Since
 286 we are shifting the probability mass for unsatisfying actions, it is possible that they are still chosen
 287 and lead to a violation. However, this is a tradeoff that we allow to achieve a given task objective.
 288 We note that this still ensures higher STL satisfaction than unconstrained actions.
 289

290 4 EVALUATION

292 4.1 IMPLEMENTATIONAL DETAILS

294 We comprehensively evaluate our constrained decoding framework on procedurally generated AI2-
 295 THOR (Kolve et al., 2022) indoor scenes with diverse objects and layouts using three state-of-
 296 the-art (SOTA) generalist robot policies: Shortest Path Oracle Clone (SPOC) (Ehsani et al., 2024),
 297 PoliFormer (Zeng et al., 2025) and Flare (Hu et al., 2025). All three are large transformer-based
 298 embodied agents trained on extensive language-conditioned robot trajectory datasets. These models
 299 achieve strong zero-shot generalization for a vast variety of navigation tasks that span open vocab-
 300 ular object-goal navigation (“find a mug”), room-to-room traversal (“visit all rooms”), waypoint-
 301 based navigation (“move three meters forward and stop near the red rug”), and attribute-conditioned
 302 variants (“locate the chair closest to the refrigerator in the kitchen”). These models also demonstrate
 303 reliable zero-shot transfer to real-world environments, achieving robust task satisfaction.
 304

305 In addition, these models capture three different training paradigms for generalist robot policies.
 306 SPOC is trained purely with imitation learning from shortest-path rollouts. Poliformer employs a
 307 hybrid approach that combines reinforcement learning and imitation learning, enabling it to learn
 308 long-horizon structure while retaining expert priors. Flare adopts a large-scale pretraining plus fine-
 309 tuning on embodied navigation data in line with recent foundation model training paradigms. This
 310 diversity in training paradigms allows us to evaluate the applicability of SafeDec across different
 311 learning regimes.

312 In this work, we address safety specifications for robotics and, therefore, select those most rel-
 313 evant to real-world deployment. In particular, we focus on an important class of safety spec-
 314 ifications called *invariants*, which are specifications that must be enforced at every reachable
 315 state of the system (e.g., “always avoid an unsafe region”). We enforce *geofencing* and *ob-
 316 stacle avoidance* by encoding them as invariant specifications in STL. Specifically, we gener-
 317 ate random regions in the configuration space that the robot must either avoid (obstacle zones)
 318 or remain within (safe zones), and apply these constraints in real time during execution. The
 319 specifications used are: $\varphi_{\text{geofence}} = \mathbf{G}(\bigvee_{i=1}^N (x_i^{\text{L}} \leq x \leq x_i^{\text{U}} \wedge z_i^{\text{L}} \leq z \leq z_i^{\text{U}}))$, $\varphi_{\text{avoid}} =$
 $\mathbf{G}(\bigwedge_{i=1}^N \neg(x_i^{\text{L}} \leq x \leq x_i^{\text{U}} \wedge z_i^{\text{L}} \leq z \leq z_i^{\text{U}}))$. The size of the regions for φ_{avoid} is 1 m^2 . For
 $\varphi_{\text{geofence}}$, we randomly pick a subset of rooms in each house and use each chosen room’s full
 320 bounds. These safety specifications are common for robot learning applications (He et al., 2024;
 321 Yun et al., 2025; Kapoor et al., 2025b; Zhao et al., 2024). We encode our test STL specifications
 322 using an efficient computational graph-based STL library called STLCG++ that can evaluate mul-
 323 tiple state signals in parallel (Kapoor et al., 2025c). This ensures minimal inference overhead at

Decoding	ϕ_{avoid} : STL / SR (% ↑)			ϕ_{geofence} : STL / SR (% ↑)		
	SPOC	Flare	PoliFormer	SPOC	Flare	PoliFormer
Unconstrained	72.0 / 82.5	75.5 / 82.0	77.0 / 82.5	78.0 / 81.5	68.0 / 81.0	73.0 / 81.5
Filtering	100.0 / 72.0	100.0 / 78.5	100.0 / 75.5	100.0 / 72.0	100.0 / 66.5	100.0 / 67.5
HCD	100.0 / 72.5	100.0 / 81.0	100.0 / 78.5	100.0 / 76.5	100.0 / 67.5	100.0 / 72.5
RCD	93.0 / 76.0	83.0 / 82.5	87.5 / 83.5	95.5 / 80.0	80.0 / 71.5	85.5 / 77.5

324
325
326
327
328
329
330
331
332
333
334
335
336
337
338
339
340
341
342
343
344
345
346
347
348
349
350
351
352
353
354
355
356
357
358
359
360
361
362
363
364
365
366
367
368
369
370
371
372
373
374
375
376
377
Table 1: Comparison by decoding technique across models (SPOC, FLARE, PoliFormer) for specifications ϕ_{avoid} and ϕ_{geofence} . Each cell reports STL satisfaction / success rate (%). Higher is better (↑).

runtime (10^{-5} s per timestep), which is crucial for policy deployment. For our dynamics model, we assume a unicycle model, an approximate first-order dynamics abstraction widely used in the robotics literature for analysis and control (Cohen et al., 2024). This representation captures the essential kinematics of motion in the plane and is widely used because it is applicable for diverse robotic platforms.

4.2 EXPERIMENTAL SETUP

We compare our proposed techniques with (1) an unconstrained base model and (2) a base model with a filtering mechanism. The filtering mechanism picks a default action (turning left or right in place) upon predicted violation of the safety specification, similar to the Simplex architecture (Sha, 2001). Simplex architecture is a classic scheme in which a high-performance advanced controller is continuously monitored by a provably safe but less capable backup controller. Simplex based techniques have been used extensively for safety-critical robotics and are a widely accepted standard for runtime-safety comparisons. We evaluate performance using two main metrics: STL Satisfaction Rate (**STL St**), defined as the proportion of trajectories that satisfy the specified STL formula, and Task Success Rate (**SR**), which measures standard task success. The three main research questions we investigated in this paper:

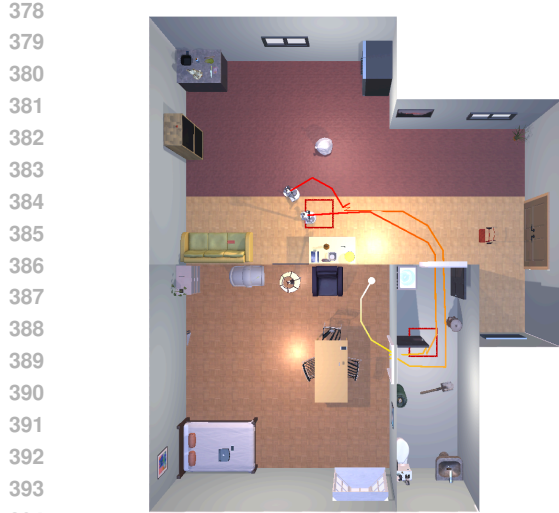
1. **RQ1:** Do HCD and RCD provide higher STL satisfaction than the unconstrained baselines?
2. **RQ2:** Do HCD and RCD preserve task success rates comparable to the unconstrained baselines?
3. **RQ3:** Does RCD achieve better task success than HCD while maintaining high STL satisfaction?

4.3 RESULTS

Our results are highlighted in Table 1. We also visualize sample trajectories in Figure 2 for one scene and task. Unless stated otherwise, all numbers are averaged over 200 evaluation episodes.

RQ1 – STL satisfaction. Both HCD and RCD consistently improve STL satisfaction relative to the unconstrained baselines across all models. For ϕ_{avoid} , unconstrained controllers achieve 72–77% satisfaction, while HCD raises this to 100% and RCD achieves 83–93%. For ϕ_{geofence} , the gap is even larger: unconstrained models reach only 68–78%, whereas HCD attains perfect compliance (100 %) in all cases and RCD achieves 80–95%. We observe that the Simplex-style filtering baseline achieves similar STL-satisfaction rate as HCD, 97 % for ϕ_{avoid} and 100 % ϕ_{geofence} . This parity is expected as both methods block any action predicted to violate the specification.

RQ2 – Task completion. Simplex-style filtering attains high satisfaction but sacrifices task success because the agent takes predefined safe actions. HCD shows similar behavior: although safety is maximized, success rates are consistently 5–10% lower than the baseline across models and specifications. However, as HCD factors in base model logits, it is able to achieve higher task satisfaction compared to Simplex-style filtering. In contrast, RCD preserves success rates much closer to the unconstrained level. For ϕ_{avoid} , RCD achieves 82–85% success compared to 82–83% for the unconstrained controllers for Flare and PoliFormer. For ϕ_{geofence} , it maintains 77–80% compared to 81–82% unconstrained for SPOC and PoliFormer. However, we note that RCD does not fully



378
379
380
381
382
383
384
385
386
387
388
389
390
391
392
393
394
395 (a) Unconstrained v/s HCD



(b) Unconstrained v/s RCD

396
397 Figure 2: Qualitative comparison of decoded trajectories for a sample scene. Each plot shows a top
398 down view of an overlay of trajectories starting from the white dot under the instruction “find an
399 alarm clock”. The unconstrained model passes through two forbidden regions (red squares) on the
400 way to the target object located on the table. In contrast, HCD (left) and RCD (right) modify the
401 trajectories to respect STL safety specifications while still reaching the goal. More visualizations
402 are available in the Appendix A.2.

403
404 recover success in every case: on SPOC with ϕ_{avoid} and Flare with ϕ_{geofence} , task success remains
405 several points below the unconstrained baseline. Nevertheless, RCD enforces safety while avoiding
406 the large performance penalty observed with filtering.

407
408 **RQ3 – RCD vs. HCD.** While both HCD and RCD improve safety over the unconstrained baseline,
409 they differ in how they balance constraint satisfaction with task success. HCD enforces strict STL
410 satisfaction that results in frequent conservatism and lower successful task completion rates. In
411 contrast, RCD’s soft penalization leads to higher task success while still maintaining reasonable
412 STL satisfaction. These results show that RCD achieves a better trade-off between safety and goal-
413 directed behavior, especially in settings where occasional low-risk actions can lead to higher long-
414 term rewards.

415 Overall, Our proposed techniques effectively enforce safety STL specifications during policy execu-
416 tion. HCD ensures full compliance, but occasionally sacrifices task success due to strict truncation.
417 RCD strikes a balance, offering high satisfaction rates and robust performance. This highlights the
418 feasibility of combining learning-based models with formal safety constraints.

420 4.4 ABLATION STUDIES

422 **Does inaccurate dynamics modeling substantially reduce STL satisfaction?** In this work, we
423 assume a simple unicycle dynamics model due it’s generalization capability for diverse robotic plat-
424 forms. Although this represents a high-level abstraction of true dynamics, such modeling simpli-
425 fications are standard in the formally assured robot safety literature (Cohen et al., 2024). However,
426 both RCD and HCD depend on this assumption and inaccurate modeling can impact STL satis-
427 faction. To evaluate the impact of inaccurate dynamics modeling, we conducted an ablation in which
428 we inject gaussian perturbations into the dynamics (0.01 m per step translational noise i.e. 5% of
429 nominal forward step, 1 ° per step rotational noise i.e. 3.3% of yaw step) for both HCD and RCD.
430 Our results are visualized in Figure 3. Across all three base models, the drop in STL satisfaction
431 rates from baseline to noisy dynamics is relatively small. We observe that SafeDec shows graceful
degradation under significant per-step disturbances.

432
433
434
435
436
437
438
439
440
441
442
443
444
445
446
447
448
449
450
451
452
453
454
455
456
457
458
459
460
461
462
463
464
465
466
467
468
469
470
471
472
473
474
475
476
477
478
479
480
481
482
483
484
485

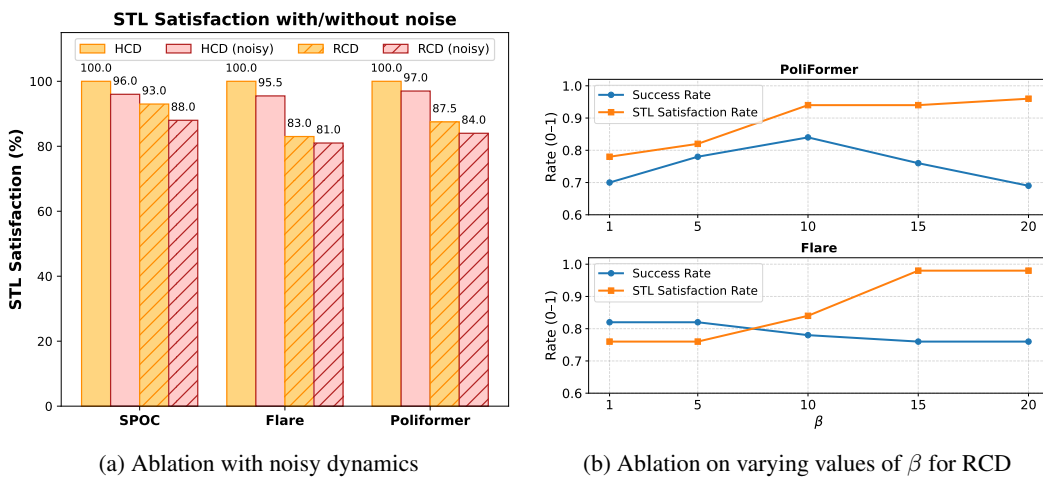


Figure 3: **Ablation studies.** (a) STL satisfaction (%) for HCD and RCD under baseline vs noisy dynamics across base models. (b) Effect of β on success rate and safety satisfaction.

How do varying values of β affect success rate and STL satisfaction in RCD? As highlighted in section 3.3, RCD uses a hyperparameter β that modulates the trade-off between specification adherence and the original task objective. The value of β affects the relative weighting between robustness and base logits. To investigate the impact of β on the success rate and STL satisfaction, we performed an ablation with varying values for β for Flare and PoliFormer. We observe that as β increases for PoliFormer, both STL satisfaction and success rate improve in tandem until $\beta = 10$, suggesting that moderate regularization can actually aid policy execution. Beyond this, STL satisfaction continues to improve but at the cost of lower success rates. For Flare, larger β values improve STL satisfaction but reduce success rates. These results highlight that the influence of β is model-dependent but in general demonstrate that SafeDec provides a tunable mechanism to balance safety and performance objectives.

5 RELATED WORK

Constraint satisfaction for robotics has been an active area of research that involves techniques such as control barrier functions (CBFs) (Ames et al., 2019), safe reinforcement learning (Gu et al., 2024), and temporal logic-based shielding approaches (Alshiekh et al., 2017). Recently, with the advent of vision language action models and their impressive generalizable capabilities for manipulation, navigation and other tasks, there are growing concerns about ensuring safety and correctness without retraining these large models. Although classical methods offer formal guarantees, they either require pretraining/fine-tuning stage interventions or designing a new classical controller for each safety specification, which can be restrictive. For example, SafeVLA (Zhang et al., 2025) fine-tunes pre-trained foundation models with task-specific safety costs, achieving strong performance in Safety-CHORES tasks. However, the safety specification is expected to be embedded in the training data and loss, meaning the model cannot generalize to new safety constraints at test time. In contrast, ASIMOV (Sermanet et al., 2025) explores rewriting dangerous instructions with better human-aligned alternatives to steer model behavior without modifying model parameters, but lacks trajectory-level formal guarantees. Our technique achieves a middle ground with the ability to adapt to novel specifications at test time without modifying model parameters while requiring minimal assumptions about the underlying model. The closest to our work is SELP (Wu et al., 2025) that proposes LTL-constrained decoding for language model-based plan generation. However, SELP is unsuitable for STL because its Boolean predicate-based LTL cannot encode numeric bounds (e.g. $\|x - x_{goal}\| < 0.1m$) and does not possess quantitative semantics, which is crucial for ranking actions. These techniques are also tailored to high-level plans from LLMs, not to the per-step low-level actions generated online by policies.

486 6 LIMITATIONS AND FUTURE WORK 487

488 In this work, we introduce a constrained decoding framework for enforcing safety specifications for
489 large transformer based robot policies. Our approach enables runtime adaptation to novel safety
490 specifications without retraining. Through experiments across multiple simulated environments, we
491 demonstrated that our method significantly improves STL satisfaction while maintaining high task
492 success rates. Our approach makes two critical assumptions that can be a limiting factor. First, we
493 assume access to specifications that are defined over the state space and that these specifications
494 are generated by roboticists. Although this is a common situation for safety critical deployment
495 contexts like aerial robotics (Aloor et al., 2023; Luckcuck et al., 2019), these specifications can
496 be difficult to design and involve access to a localization module that can provide accurate state
497 estimation. We plan to overcome this bottleneck by leveraging open-world safety specifications
498 using recent work on embedding spaces-based logic (Kapoor et al., 2025a) and using large language
499 models for generating high level specifications automatically (Li et al., 2025). Second, our approach
500 also assumes access to an approximate dynamics model to evaluate the impact of actions on future
501 trajectories. While a common assumption for provably safe robotics (Cohen et al., 2024), This can
502 limit applicability of our approach. However, it is possible to mitigate this via learned dynamics
503 models such as MoSim (Hao et al., 2025) or world models proposed in Zhou et al. (2025); Micheli
504 et al. (2023) and we plan to explore this in future work.

505 REFERENCES 506

507 Guidance AI. Guidance: A language model control framework. <https://github.com/guidance-ai/guidance>, 2023. Accessed: April 27, 2025.

510 Jasmine Jerry Aloor, Jay Patrikar, Parv Kapoor, Jean Oh, and Sebastian Scherer. Follow the rules:
511 Online signal temporal logic tree search for guided imitation learning in stochastic domains. In
512 *2023 IEEE International Conference on Robotics and Automation (ICRA)*, pp. 1320–1326, 2023.
513 doi: 10.1109/ICRA48891.2023.10160953.

514 Mohammed Alshiekh, Roderick Bloem, Ruediger Ehlers, Bettina Könighofer, Scott Niekum, and
515 Ufuk Topcu. Safe reinforcement learning via shielding, 2017. URL <https://arxiv.org/abs/1708.08611>.

518 Aaron D. Ames, Samuel Coogan, Magnus Egerstedt, Gennaro Notomista, Koushil Sreenath, and
519 Paulo Tabuada. Control barrier functions: Theory and applications, 2019. URL <https://arxiv.org/abs/1903.11199>.

521 Luca Beurer-Kellner, Marc Fischer, and Martin Vechev. Prompting is programming: A query
522 language for large language models. *Proc. ACM Program. Lang.*, 7(PLDI), June 2023. doi:
523 10.1145/3591300. URL <https://doi.org/10.1145/3591300>.

525 Max H. Cohen, Tamas G. Molnar, and Aaron D. Ames. Safety-critical control for autonomous sys-
526 tems: Control barrier functions via reduced-order models. *Annual Reviews in Control*, 57:100947,
527 2024. ISSN 1367-5788. doi: <https://doi.org/10.1016/j.arcontrol.2024.100947>. URL <https://www.sciencedirect.com/science/article/pii/S1367578824000166>.

530 Kiana Ehsani, Tanmay Gupta, Rose Hendrix, Jordi Salvador, Luca Weihs, Kuo-Hao Zeng, Ku-
531 nal Pratap Singh, Yejin Kim, Winson Han, Alvaro Herrasti, et al. Spoc: Imitating shortest paths
532 in simulation enables effective navigation and manipulation in the real world. In *Proceedings of*
533 *the IEEE/CVF Conference on Computer Vision and Pattern Recognition*, pp. 16238–16250, 2024.

534 Angela Fan, Mike Lewis, and Yann Dauphin. Hierarchical neural story generation. *arXiv preprint*
535 *arXiv:1805.04833*, 2018.

537 Marie Farrell, Matt Luckcuck, and Michael Fisher. *Robotics and Integrated Formal Methods:*
538 *Necessity Meets Opportunity*, pp. 161–171. Springer International Publishing, 2018. ISBN
539 9783319989389. doi: 10.1007/978-3-319-98938-9_10. URL http://dx.doi.org/10.1007/978-3-319-98938-9_10.

540 Shangding Gu, Long Yang, Yali Du, Guang Chen, Florian Walter, Jun Wang, and Alois Knoll. A
541 review of safe reinforcement learning: Methods, theory and applications, 2024. URL <https://arxiv.org/abs/2205.10330>.
542

543 Chenjie Hao, Weyl Lu, Yifan Xu, and Yubei Chen. Neural motion simulator: Pushing the limit
544 of world models in reinforcement learning, 2025. URL <https://arxiv.org/abs/2504.07095>.
545

546 Tairan He, Chong Zhang, Wenli Xiao, Guanqi He, Changliu Liu, and Guanya Shi. Agile but safe:
547 Learning collision-free high-speed legged locomotion. In *Robotics: Science and Systems (RSS)*,
548 2024.
549

550 Chris Hokamp and Qun Liu. Lexically constrained decoding for sequence generation using
551 grid beam search. In Regina Barzilay and Min-Yen Kan (eds.), *Proceedings of the 55th An-
552 nual Meeting of the Association for Computational Linguistics (Volume 1: Long Papers)*, pp.
553 1535–1546, Vancouver, Canada, July 2017. Association for Computational Linguistics. doi:
554 10.18653/v1/P17-1141. URL <https://aclanthology.org/P17-1141/>.
555

556 Ari Holtzman, Jan Buys, Li Du, Maxwell Forbes, and Yejin Choi. The curious case of neural text
557 degeneration. *arXiv preprint arXiv:1904.09751*, 2019.
558

559 Jiaheng Hu, Rose Hendrix, Ali Farhadi, Aniruddha Kembhavi, Roberto Martín-Martín, Peter Stone,
560 Kuo-Hao Zeng, and Kiana Ehsani. Flare: Achieving masterful and adaptive robot policies
561 with large-scale reinforcement learning fine-tuning. In *2025 IEEE International Conference on
562 Robotics and Automation (ICRA)*, pp. 3617–3624. IEEE, 2025.

563 Yafei Hu, Quanting Xie, Vidhi Jain, Jonathan Francis, Jay Patrikar, Nikhil Varma Keetha, Seungchan
564 Kim, Yaqi Xie, Tianyi Zhang, Shibo Zhao, et al. Toward general-purpose robots via foundation
565 models: A survey and meta-analysis. *CoRR*, 2023.
566

567 Parv Kapoor, Sai Vemprala, and Ashish Kapoor. Logically constrained robotics transformers for
568 enhanced perception-action planning. *arXiv preprint arXiv:2408.05336*, 2024.
569

570 Parv Kapoor, Abigail Hammer, Ashish Kapoor, Karen Leung, and Eunsuk Kang. Pretrained em-
571 beddings as a behavior specification mechanism, 2025a. URL <https://arxiv.org/abs/2503.02012>.
572

573 Parv Kapoor, Ian Higgins, Nikhil Keetha, Jay Patrikar, Brady Moon, Zelin Ye, Yao He, Ivan Cis-
574 neros, Yaoyu Hu, Changliu Liu, Eunsuk Kang, and Sebastian Scherer. Demonstrating visafe:
575 Vision-enabled safety for high-speed detect and avoid. 2025b.
576

577 Parv Kapoor, Kazuki Mizuta, Eunsuk Kang, and Karen Leung. Stlcg++: A masking approach
578 for differentiable signal temporal logic specification. *IEEE Robotics and Automation Letters*,
579 10(9):9240–9247, September 2025c. ISSN 2377-3774. doi: 10.1109/LRA.2025.3588389. URL
580 <http://dx.doi.org/10.1109/LRA.2025.3588389>.
581

582 Moo Jin Kim, Karl Pertsch, Siddharth Karamcheti, Ted Xiao, Ashwin Balakrishna, Suraj Nair,
583 Rafael Rafailov, Ethan Foster, Grace Lam, Pannag Sanketi, Quan Vuong, Thomas Kollar, Ben-
584 jamin Burchfiel, Russ Tedrake, Dorsa Sadigh, Sergey Levine, Percy Liang, and Chelsea Finn.
585 Openvla: An open-source vision-language-action model, 2024. URL <https://arxiv.org/abs/2406.09246>.
586

587 Eric Kolve, Roozbeh Mottaghi, Winson Han, Eli VanderBilt, Luca Weihs, Alvaro Herrasti, Matt
588 Deitke, Kiana Ehsani, Daniel Gordon, Yuke Zhu, Aniruddha Kembhavi, Abhinav Gupta, and Ali
589 Farhadi. Ai2-thor: An interactive 3d environment for visual ai, 2022. URL <https://arxiv.org/abs/1712.05474>.
590

591 Manling Li, Shiyu Zhao, Qineng Wang, Kangrui Wang, Yu Zhou, Sanjana Srivastava, Cem Gokmen,
592 Tony Lee, Li Erran Li, Ruohan Zhang, Weiyu Liu, Percy Liang, Li Fei-Fei, Jiayuan Mao, and
593 Jiajun Wu. Embodied agent interface: Benchmarking llms for embodied decision making, 2025.
594 URL <https://arxiv.org/abs/2410.07166>.

594 Alisa Liu, Maarten Sap, Ximing Lu, Swabha Swayamdipta, Chandra Bhagavatula, Noah A. Smith,
595 and Yejin Choi. Dexperts: Decoding-time controlled text generation with experts and anti-experts,
596 2021. URL <https://arxiv.org/abs/2105.03023>.

597 Matt Luckcuck, Marie Farrell, Louise A. Dennis, Clare Dixon, and Michael Fisher. Formal spec-
598 ification and verification of autonomous robotic systems: A survey. *ACM Computing Sur-
599 veys*, 52(5):1–41, September 2019. ISSN 1557-7341. doi: 10.1145/3342355. URL <http://dx.doi.org/10.1145/3342355>.

600 O. Maler and D. Nickovic. Monitoring Temporal Properties of Continuous Signals. (3253):152–166,
601 2004a.

602 Oded Maler and D. Nickovic. Monitoring temporal properties of continuous signals. In
603 *FORMATS/FTRTFT*, 2004b. URL <https://api.semanticscholar.org/CorpusID:15642684>.

604 Claudio Menghi, Christos Tsigkanos, Patrizio Pelliccione, Carlo Ghezzi, and Thorsten Berger. Spec-
605 ification patterns for robotic missions. *CoRR*, abs/1901.02077, 2019. URL <http://arxiv.org/abs/1901.02077>.

606 Vincent Micheli, Eloi Alonso, and François Fleuret. Transformers are sample-efficient world
607 models. In *The Eleventh International Conference on Learning Representations*, 2023. URL
608 <https://openreview.net/forum?id=vhFu1Acb0xb>.

609 Kanghee Park, Jiayu Wang, Taylor Berg-Kirkpatrick, Nadia Polikarpova, and Loris D' An-
610 toni. Grammar-aligned decoding. In A. Globerson, L. Mackey, D. Belgrave,
611 A. Fan, U. Paquet, J. Tomczak, and C. Zhang (eds.), *Advances in Neural In-
612 formation Processing Systems*, volume 37, pp. 24547–24568. Curran Associates, Inc.,
613 2024. URL https://proceedings.neurips.cc/paper_files/paper/2024/file/2bdc2267c3d7d01523e2e17ac0a754f3-Paper-Conference.pdf.

614 Maxime Peyrard, Martin Josifoski, and Robert West. The era of semantic decoding, 2024. URL
615 <https://arxiv.org/abs/2403.14562>.

616 Amir Pnueli. The temporal logic of programs. In *18th Annual Symposium on Foundations of
617 Computer Science (sfcs 1977)*, pp. 46–57, 1977. doi: 10.1109/SFCS.1977.32.

618 Pierre Sermanet, Anirudha Majumdar, Alex Irpan, Dmitry Kalashnikov, and Vikas Sindhwani. Gen-
619 erating robot constitutions & benchmarks for semantic safety. *arXiv preprint arXiv:2503.08663*,
620 2025.

621 Lui Sha. Using simplicity to control complexity. *IEEE Software*, 18(4):20–28, 2001. doi: 10.1109/MS.2001.936213.

622 Sean Welleck, Amanda Bertsch, Matthew Finlayson, Hailey Schoelkopf, Alex Xie, Graham Neubig,
623 Ilia Kulikov, and Zaid Harchaoui. From decoding to meta-generation: Inference-time algorithms
624 for large language models, 2024. URL <https://arxiv.org/abs/2406.16838>.

625 Brandon T Willard and Rémi Louf. Efficient guided generation for large language models. *arXiv
626 preprint arXiv:2307.09702*, 2023.

627 Yi Wu, Zikang Xiong, Yiran Hu, Shreyash S. Iyengar, Nan Jiang, Aniket Bera, Lin Tan, and Suresh
628 Jagannathan. Selp: Generating safe and efficient task plans for robot agents with large language
629 models, 2025. URL <https://arxiv.org/abs/2409.19471>.

630 Kai S Yun, Rui Chen, Chase Dunaway, John M Dolan, and Changliu Liu. Safe control of quadruped
631 in varying dynamics via safety index adaptation. In *2025 IEEE International Conference on
632 Robotics and Automation (ICRA)*, pp. 7771–7777. IEEE, 2025.

633 Kuo-Hao Zeng, Zichen Zhang, Kiana Ehsani, Rose Hendrix, Jordi Salvador, Alvaro Herrasti, Ross
634 Girshick, Aniruddha Kembhavi, and Luca Weihs. Poliformer: Scaling on-policy rl with trans-
635 formers results in masterful navigators. In *Conference on Robot Learning*, pp. 408–432. PMLR,
636 2025.

648 Borong Zhang, Yuhao Zhang, Jiaming Ji, Yingshan Lei, Josef Dai, Yuanpei Chen, and Yaodong
 649 Yang. Safevla: Towards safety alignment of vision-language-action model via safe reinforcement
 650 learning, 2025. URL <https://arxiv.org/abs/2503.03480>.

651
 652 Weiye Zhao, Yifan Sun, Feihan Li, Rui Chen, Ruixuan Liu, Tianhao Wei, and Changliu
 653 Liu. GUARD: A safe reinforcement learning benchmark. *Transactions on Machine Learn-
 654 ing Research*, 2024. ISSN 2835-8856. URL <https://openreview.net/forum?id=kZFKwApeQO>.

655
 656 Gaoyue Zhou, Hengkai Pan, Yann LeCun, and Lerrel Pinto. Dino-wm: World models on pre-
 657 trained visual features enable zero-shot planning, 2025. URL <https://arxiv.org/abs/2411.04983>.

658
 659
 660

A APPENDIX

A.1 QUANTITATIVE SEMANTICS OF STL

Given a signal s_t representing a signal starting at time t , the quantitative semantics of satisfaction of $s_t \models \phi$ are defined inductively as follows:

$$\begin{aligned}\rho(s_t, \mu_c) &= \mu(x_t) - c \\ \rho(s_t, \neg\varphi) &= -\rho(s_t, \varphi) \\ \rho(s_t, \varphi_1 \wedge \varphi_2) &= \min(\rho(s_t, \varphi_1), \rho(s_t, \varphi_2)) \\ \rho(s_t, F_{[a,b]}(\varphi)) &= \max_{t' \in [t+a, t+b]} \rho(s_{t'}, \varphi) \\ \rho(s_t, G_{[a,b]}(\varphi)) &= \min_{t' \in [t+a, t+b]} \rho(s_{t'}, \varphi)\end{aligned}$$

A.2 VISUALIZATIONS

To complement our quantitative results, we provide numerous trajectory plots from evaluations across a diverse set of procedurally generated indoor environments. Figure 4 illustrates representative top-down visualizations of trajectories induced by `SafeDec`. Each plot shows the agent's starting point and the resulting path under constrained decoding, with red circles marking target objects, green boxes denoting forbidden regions, and orange paths depicting the safe trajectories generated by our method. Together with our quantitative analysis, these qualitative results illustrate the performance of `SafeDec` across environments and tasks.



Figure 4: Top-down views across indoor environments with `SafeDec` induced trajectories. Red circles mark target objects, green boxes are avoid regions, and orange paths show safe trajectories under constrained decoding.